Electronic Supplementary Material (ESI) for Materials Advances.

Electronic Supplementary Information

Preparation of ultra-low profile and high peel strength copper foil with rice-grain microstructure

Li-juan Wang, Xiao-wei Fa, Yun-zhi Tang*, Juan Liao, Yu-hui Tan*, Ning Song, Jian Huang, Zhen Sun, Men Zhao, Wei-fei Liu, Man Zhao

Table.S1 Electrolyte composition for different procedures

Composition	Electroplating solution	Micro-coarsening solution	Curing solution	heat resistant alloy treatment	Silane coupling solution
$CuSO_4 \cdot 5H_2O$(g/L)	70	10	40		—
H_2SO_4(g/L)	120	100	100		—
HCl(ppm/L)	15	—	—		—
Additive 1(mg/L)	10	—	—		—
Additive 2(mg/L)	20	—	—		—
$Na_2WO_4 \cdot 2H_2O$(g/L)	—	0.05	—	40	—
$Tb_2(SO_4)_3 \cdot 8H_2O$(g/L)	—	0.1	—		—
KH 590(mL/L)	—	—	—		2
$NiSO_4 \cdot 7H_2O$(g/L)				20	
$C_6H_5Na_3O_7$(g/L)				40	
$(NH_4SO_4)_2SO_4$(g/L)				15	

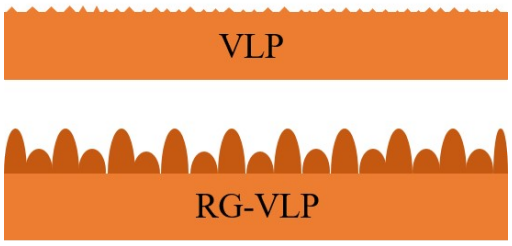

Fig. S1. Schematic diagram of two different copper tumor after coarsening treatment for **VLP** and **RG-VLP**

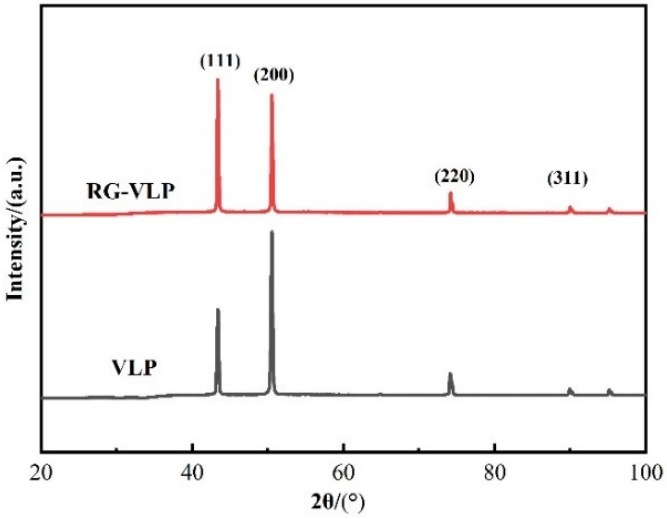

Fig. S2. XRD of copper foil before and after micro-coarsening

Table.S2 Crystal orientation T_C (%) and grain size D* of copper foil before and after micro-coarsening.

Samples	$T_{c(111)}$	$T_{c(200)}$	$T_{c(220)}$	$T_{c(311)}$	D*/nm
VLP	14.17	59.22	20.84	5.77	—
RG-VLP	26.40	51.77	15.31	6.52	30.51

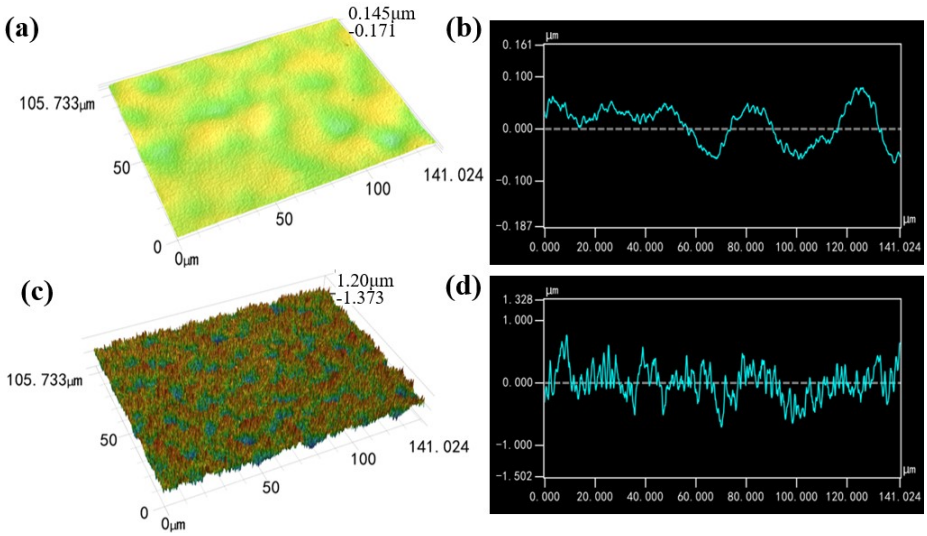

Fig. S3. 3D morphology of copper foil surface and cross-sectional change for (a) (b)**VLP** and (c) (d) **RG-VLP** respectively

Table S2 CLSM values for copper foils.

Sample	Rz (μm)	Ra (μm)	Surface area (μm^2)	Surface area ratio
VLP	0.995	0.117	18512.53	1.09
RG-VLP	1.887	0.264	24010.62	1.44

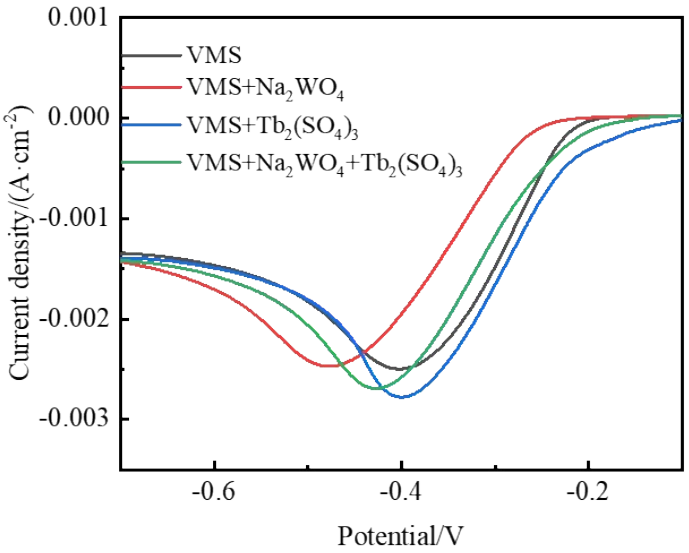

Fig. S4. Polarization curves of additives in roughening solution

The additive Na_2WO_4 shifted the polarization curve negatively when added to the blank solution, acting as an inhibitor of copper ion deposition. The additive $Tb_2(SO_4)_3$ shifted the polarization curve positively when added to the blank solution, acting to promote the deposition of copper ions. The synergistic effect of the two additives plays a polarizing effect, inhibiting the deposition of copper ions, which is conducive to controlling the morphology and size of copper tumors.

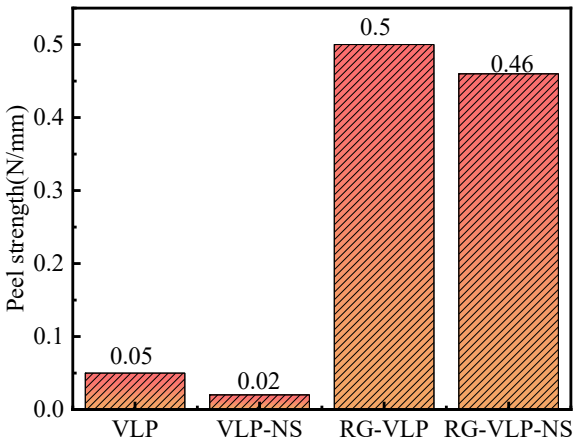

Fig. S5. Peel strength of copper foil (Note: VLP-NS, RG-VLP-NS indicate without silane treatment)

The peel strength of VLP-NS was reduced by 0.03 N/mm compared to VLP, and the peel strength of RG-VLP-NS was reduced by 0.04 N/mm compared to RG-VLP.

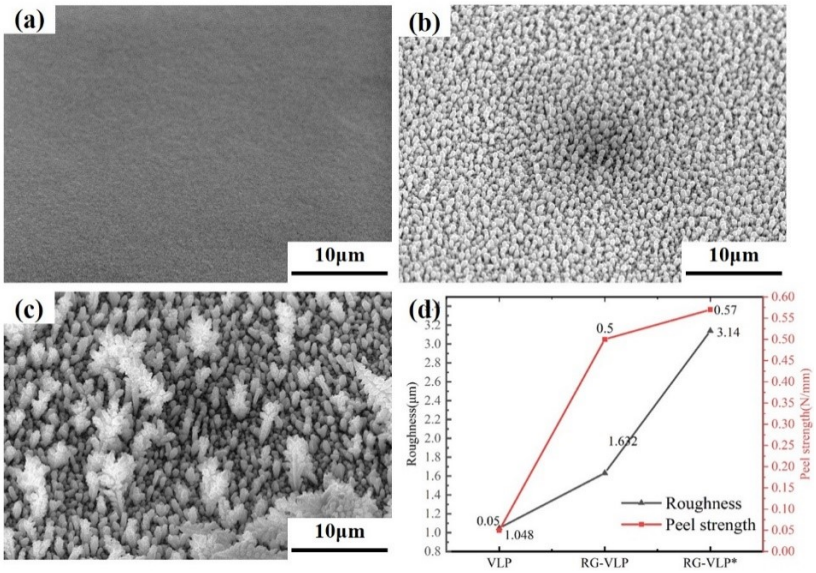

Fig. S6. The SEM and performance test plots of copper foils, (a) VLP, (b) RG-VLP, (c) RG-VLP*, (d) surface roughness and peel strength of copper foils.

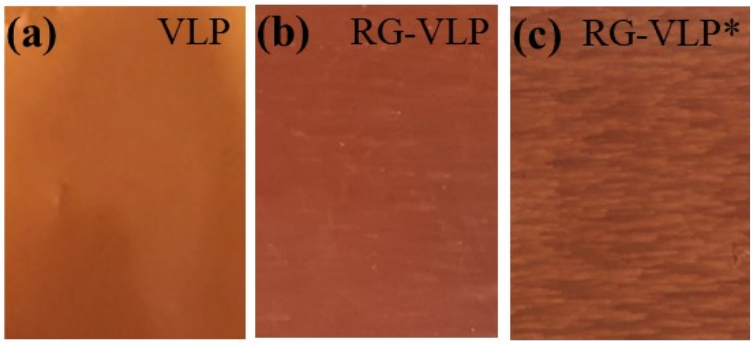

Fig. S7. The physical photographs of copper foil, (a) VLP, (b) RG-VLP, (c) RG-VLP*

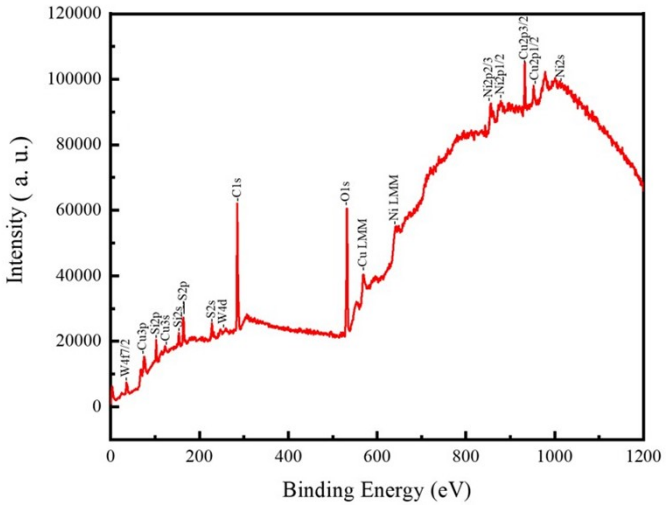

Fig. S8. XPS analysis spectrum of copper foil surface

Fig. S8 shows the XPS analysis spectrum of the VLP surface, and the peaks of Si_{2p} and Si_{2s} were detected at 102.40 eV and 153.46 eV, respectively. In addition, the presence of silane coupling agent on the surface of the copper foil was also verified by the detection of the peak of S_{2p} in sulfhydryl group at 163.76 eV. The W_{4f} has a peak value at 34.88eV between 34.75 and 35.58eV, which proves that the copper foil surface contains W element. The binding energies of Ni_{2p} are in the range of 853.28-853.3 eV and 855.08-855.3 eV, and the peak at 855.76 eV in the figure indicates the presence of Ni element on the surface of the copper foil.